ON THE ANALYSIS OF MCM SYSTEMS PAPR PROFILES AND THE WP-OFDM SYSTEM PAPR REDUCTION TECHNIQUES

JAMALUDDIN BIN ZAKARIA

UNIVERSITI SAINS MALAYSIA

2013

ON THE ANALYSIS OF MCM SYSTEMS PAPR PROFILES AND THE WP-OFDM SYSTEM PAPR REDUCTION TECHNIQUES

by

JAMALUDDIN BIN ZAKARIA

Thesis submitted in fulfilment of the requirements
for the degree of
Master of Science

June 2013

ACKNOWLEDGEMENTS

In the Name of Allah, the Most Beneficent, the Most Merciful.

All praises only to Allah s.w.t. who the Creator of mankind and universe, which allow me to complete all my studies and works in this Master of Science degree. Only along His permission, this effort of thesis and works completion can be done successfully.

A warmly gratitude and appreciation to my dedicated supervisor, Assoc. Prof. Dr. Mohd. Fadzli bin Mohd. Salleh who always give me guidance, ideas, motivations and support for the project. He helps me to visualize and identify better approaches in problem solving. He also encourages me to publish my works and this speeds up my research and thesis writing.

A special appreciation to my beloved parents, Mr. Zakaria bin Ab. Rahim and Mdm. Saidah binti Saad. Thank you for allowing me to pursue my study until to this level.

Thanks to all USM staffs especially to School of Electric and Electronic Engineering (SEE) and Institute of Postgraduate Studies (IPS) staffs. And, special thanks, tribute and appreciation to all my friends which give a supportive utterances and constructive encouragements. Thanks to all those their names do not appear here who have contributed to the successful completion of this research study.

This research is fully supported by USM RU grant, under Grant No. 1001/PELECT/814100.

TABLE OF CONTENTS

LIST OF TABLES

LIST OF FIGURES

LIST OF ABBREVIATIONS

i.i.d.	Independent and identically distributed
w.r.t.	with respect to
ACE	Active constellation extension
AWGN	Additive white Gaussian noise
BER	Bit error rate
BPSK	Binary phase shift keying
CCDF	Complementary cumulative distribution function
CDF	Cumulative distribution function
C-OFDM	Conventional orthogonal frequency division multiplexing
C-PTS	Conventional PTS
CP	Cyclic prefix
DFT	Discrete Fourier transform
DSI	Dummy sequence insertion
DWPT	Discrete wavelet packet transform
DWT	Discrete wavelet transform
FDM	Frequency division multiplexing
FT	Fourier transform
HPA	High power amplifier

ICI Intercarrier interference

IDFT Inverse discrete Fourier transform

IDWPT Inverse discrete wavelet packet transform

IDWT Inverse discrete wavelet transform

IFFT Inverse fast Fourier transform

ISI Intersymbol interference

MCM Multicarrier modulation

MRA Multi-resolution analysis

OFDM Orthogonal frequency division multiplexing

PAPR Peak-to-average power ratio

PDF Probability density function

P/S Parallel-to-serial

PSK Phase-shift-keying

PTS Partial transmit sequence

RS Reed-Solomon

QAM Quadrature amplitude modulation

QPSK Quadrature phase shift keying

SCM Single-carrier modulation

SI Side information

SLM Selected mapping

SNR Signal-to-noise ratio

S/P Serial-to-parallel

TI Tone injection

TR Tone reservation

WLAN Wireless local area network

WPM Wavelet packet modulation

WP-OFDM Wavelet packet-based OFDM

WPT Wavelet packet transform

WT Wavelet transform

WOFDM Wavelet-based OFDM

LIST OF SYMBOLS

a	Wavelet scaling parameter (used in CWT)
α	Scaling index (used in DWT)
b	Wavelet translation parameter (used in CWT)
β	Translation index (used in DWT)
$c_\alpha(\beta)$	Approximation coefficient (scaling DWT coefficients)
$d_\alpha(\beta)$	Detail coefficient (wavelet DWT coefficients)
$g(n)$	Wavelet filter (wavelet function coefficient)
$h(n)$	Scaling filter (scaling function coefficient)
$L^2(\mathbb{R})$	Vector space of square integrated function
l	Node depth of wavelet packet tree
p	Position of current node in wavelet packet
$\varphi_{\alpha,\beta}(t)$	Scaling function
$\varphi(t)$	Sum of the weighted time-shifted scaling function
v_0	Space spanned by a function
$\psi_{CWT}(t)$	Prototype mother wavelet (CWT)
$\psi_{CWT_{a,b}}(t)$	The scaled and translated version of prototype mother wavelet (CWT)
$\Psi_{CWT}(\Omega)$	Fourier transform of $\psi_{CWT}(t)$
$\psi_{\alpha,\beta}(t)$	Wavelet function

$\psi(t)$	Sum of the weighted time-shifted wavelet function
ζ_l^p	Wavelet packet coefficient (general)
ζ_{l+1}^{2p}	Wavelet packet coefficient (generated by scaling filter)
ζ_{l+1}^{2p+1}	Wavelet packet coefficient (generated by wavelet filter)
$coifN$	Coiflet wavelet (length of $2N$)
dbN	Daubechies wavelet (length of $2N$)
$db1$	Daubechies-1 wavelet (length of 2)
$dmeyN$	Discrete meyer wavelet
$symN$	Symlet wavelet (length of $2N$)
n_{final}	Number of final binary recovered information
n_{init}	Number of initial binary information
E_b/N_0	Energy bit per noise ratio
N	Number of subcarriers (per MCM frame)
N_{bps}	Number of bits per symbol
P	Maximum potential number of encoded symbols
R	Number of remaining position (unused or SI subcarriers)
$RS\{\cdot\}$	RS encoder notation
$RS^{-1}\{\cdot\}$	RS decoder notation
b^v	Value of allowable phase factor
$\tilde{b}$	Optimized value of allowable phase factor (post-defined SI)

$\tilde{\mathbf{b}}$	Sequence of optimized post-defined SI (value of allowable phase factor)
m	Integer for finding optimized phase factor
v	Number of order of disjoint subblocks per frame
w	Total number of allowable phase factor
$\dot{b}$	Integer value of SI
$\tilde{B}$	Post-defined SI index
$\tilde{\mathbf{B}}$	Sequence of post-defined SI index
M_B	Integer of post-defined SI index
V	Maximum number of disjoint subblocks (in PTS)

PADA ANALISIS PROFIL NKPP BAGI SISTEM PBP DAN TEKNIK PENGURANGAN NKPP BAGI SISTEM BGK-PPFO

ABSTRAK

Pemultipleksan Pembahagian Frekuensi Ortogon (PPFO) adalah satu sistem yang penting dalam menghantar isyarat pemodulatan berbilang pembawa (PBP) melalui saluran pemudaran memilih. Ia mempunyai beberapa ciri-ciri yang unggul seperti mampu untuk mencapai kecekapan jalur lebar yang lebih tinggi, penghantaran data yang lebih banyak, mantap terhadap gangguan frekuensi jalur sempit dan pelaksanaan yang kurang kompleks. Namun, sistem ini mempunyai kelemahan yang memerlukan penambahbaikan iaitu memiliki Nisbah Kuasa Puncak-kepada-Purata (NKPP) yang tinggi yang menyebabkan isyarat yang beroperasi di rantau tidak-lelurus bagi Penguat Kuasa Tinggi (PKT) mengalami prestasi buruk dan kecacatan isyarat yang lain. Selain daripada itu, satu perkakas yang dinamik dan menarik iaitu analisis gelombang kecil digunakan dan ia adalah terbitan dari Jelmaan Bingkisan Gelombang Kecil (JBGK) yang memiliki kriteria yang hampir sama dengan asas Fourier ortogon dalam sistem PBP. Analisis asas gelombang kecil mempunyai kelebihan berbanding asas Fourier dari segi isyarat fungsi tetingkap yang berkebolehlenturan untuk analisis isyarat tidak bergerak. Subset bagi asas JBGK dikenali sebagai Jelmaan Gelombang Kecil Diskret (JGKD). Dalam sistem PBP, kedua-dua fungsi asas tersebut membina sistem isyarat pemodulatan ortogon, sama seperti bagi Jelmaan Fourier Pantas (JFP) dalam sistem PPFO yang lazim (PPFO-L). Pelaksanaan kedua-dua JBGK dan JGKD dalam sistem umum PBP, menghasilkan masing-masing isyarat Bingkisan Gelombang Kecil-PPFO (BGK-PPFO) dan isyarat Gelombang Kecil Terasas-PPFO (GKT-PPFO). Tanpa memerlukan menggunakan awalan kitar (AK), isyarat-isyarat ortogon ini mempunyai lebar jalur yang lebih tinggi. Oleh itu, satu kajian menyeluruh dilaksanakan de-

ngan melakukan manipulasi pada parameter tertentu bagi isyarat-isyarat BGK-PPFO, GKT-PPFO dan PPFO-L melalui saluran AWGN. Tambahan pula, jujukan menghantar separa (JMS) adalah satu teknik yang berkesan bagi mengurangkan NKPP yang besar dalam isyarat BGK-PPFO. Oleh kerana maklumat sampingan (MS) terhasil dari pengoptimuman JMS, tesis ini mencadangkan dua teknik terhadap membenamkan MS ke dalam ruangan tersedia dalam kerangka data BGK-PPFO. Skim Cadangan JMS I boleh dilaksanakan dengan mudah; sehingga lapan MS dibolehkan untuk dibenamkan. Ini bermakna sehingga lapan pembahagian kecil bagi kerangka data BGK-PPFO boleh dibuat untuk pengoptimuman. Hasil yang terbaik bagi Skim Cadangan JMS I adalah pemilihan parameter 8 dan 12 masing-masing bagi bilangan pembahagian kecil dan bilangan faktor fasa yang dibenarkan. Di samping itu, Skim Cadangan JMS II melaksanakan pemodulatan kekunci anjakan fasa kepada MS sebelum dibenamkan ke dalam kerangka data BGK-PPFO. Dengan ini, bilangan pembahagian kecil lebih banyak dapat dicapai berbanding Skim Cadangan JMS I dan prestasi kadar ralat bit dapat diperbaiki. Hasil yang terbaik bagi Skim Cadangan JMS II adalah pemilihan parameter 16 dan 4 masing-masing bagi bilangan pembahagian kecil dan bilangan faktor fasa yang dibenarkan.

ON THE ANALYSIS OF MCM SYSTEMS PAPR PROFILES AND THE WP-OFDM SYSTEM PAPR REDUCTION TECHNIQUES

ABSTRACT

Orthogonal frequency division multiplexing (OFDM) is a prominent system in transmitting multicarrier modulation (MCM) signals over selective fading channel. It has several magnificent properties such as attaining a higher degree of bandwidth efficiency, higher data transmission, robust to narrowband frequency interference and low-complexity implementation. However, the system has its shortage which needs improvement; high peak-to-average power ratio (PAPR) where the signals work in the nonlinear region of the high power amplifier (HPA) results in poor performance and other signal property impairments. Apart from that, an attractive dynamic tool which is wavelet analysis is utilized, and its derivatives such as wavelet packet transform (WPT) possesses almost the same criteria of the orthogonal Fourier base MCM system. Wavelet base analysis surpasses Fourier base by inherent flexibility in terms of windows function for non-stationary signal analysis. The subset base of WPT known as discrete wavelet transforms (DWT). In MCM system, these two base functions construct the orthogonal modulation signal system as the fast Fourier transform (FFT) do in the conventional OFDM (C-OFDM) system. Applying both WPT and DWT in the MCM system, produces orthogonal signals known as the wavelet packet-based OFDM (WP-OFDM) and wavelet-based OFDM (WOFDM) signals respectively. With no cyclic prefix (CP) need to be applied, these orthogonal signals hold higher bandwidth efficiency. Hence, a comprehensive study is established by performing manipulation on specified parameters using WP-OFDM, WOFDM and C-OFDM signals under the additive white Gaussian noise (AWGN) channel. Furthermore, Partial Transmit Sequence (PTS) is an efficient technique to mitigate the large PAPR in WP-OFDM signals.

Due to side information generation from PTS optimization, this thesis proposed two techniques on embedding the side information (SI) generation into provided space positions within WP-OFDM frame. The Proposed PTS Scheme I is a direct implementation, where at most, eight SI are allowed to be embedded. This implies that up to eight disjoint subblocks can be made for optimization. The WP-OFDM system using the first Proposed PTS Scheme obtained the best result which is 8.20dB at 10^{-4} of CCDF of PAPR and E_b/N_0 of 28dB at BER level of 10^{-6} for the chosen number of disjoint subblocks and the number of allowable phase factor is eight and twelve respectively. In addition, the Proposed PTS Scheme II implements particular degree of PSK modulation to the SI prior embeds into the provided space within the WP-OFDM frame. In general, this allows higher number of subblock than the first proposed scheme and it improves the BER performance of the scheme apparently. The best results obtained is the CCDF of PAPR is 8.35dB at 10^{-4} and E_b/N_0 of 24dB at BER level of 10^{-6} for the number of disjoint subblocks and the number of allowable phase factor is 16 and 4 respectively.

CHAPTER 1

INTRODUCTION

1.1 Preface

For the last several decades, the principle of Orthogonal Frequency Division Multiplexing (OFDM) modulation has been in existence. Many communication systems have employed this technique such as in wireless networking systems, data delivery systems over phone line and digital television and digital radio systems.

In early years of the development of modulation techniques for communication systems, single-carrier modulation (SCM) modulates information onto one carrier using amplitude, frequency or phase adjustment as shown in Figure 1.1 (a). The information is in the form of bits, or combination of bits (symbols) which modulated onto carrier. As the increasing of signal information bandwidth, the duration of one bit or symbol of information become smaller. This causes the system to be more susceptible to intersymbol interference (ISI) thus experiencing higher distortion. The receiver has the tendency of losing information due to the presence of impulse noise or unwanted signal from devices impairments. This leads to incapability to recover the received signal. As a result, the corrupted SCM signal will not provide any valuable information at that particular instant of communication.

Besides, Frequency Division Multiplexing (FDM) is another type of modulation technique which is widely used in telegraph (LaSorte et al., 2008; Weinstein, 2009). It is the extension concept of single carrier communication that uses multiple subcarriers within a specific signal bandwidth. The total data rate to be sent via the channel is divided among the subcarriers. This modulation type is categorized as the multicarrier modulation (MCM) communication

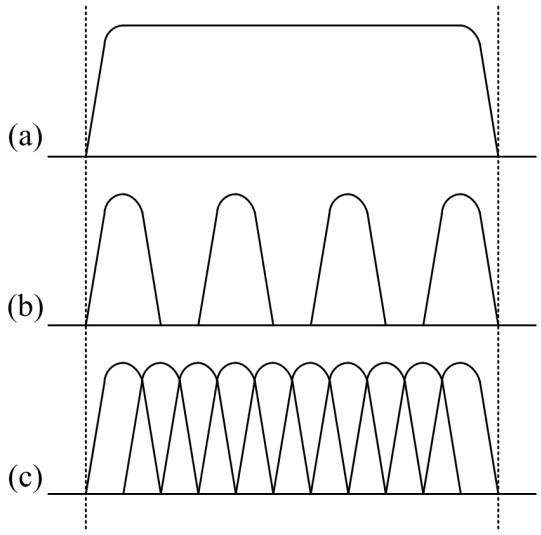

Figure 1.1: Comparison between (a) SCM, (b) FDM and (c) OFDM

class since it employs several lower rate subcarriers to carry the information as depicted in Figure 1.1 (b). FDM has advantages over SCM in term of immunity to narrowband frequency interference. Unlike SCM, FDM requires guard bands or empty spectral regions between the subcarriers in order to prevent spectral overlapping, which reduces the efficiency of delivery information or data rates under fixed range of channel bandwidth.

Observing the prospect of demanding higher data transmission rate for future generation, Chang (1966) introduces an improved FDM technique called Orthogonal FDM (OFDM) as published in (Chang, 1966). The concept of OFDM is similar to FDM where the frequency selective channel is divided into several number of frequency subchannels. Each individual subcarrier is arranged in orthogonal fashion as shown in Figure 1.1 (c) after performing Fourier transform operation. Thus the guard bands as required in FDM system are no longer needed. Although the spectra of subcarriers signals are overlapping, the information can be recovered as long as the orthogonality of the spectra is well-preserved.

Indeed, OFDM technique offers several advantages: It attains higher degree of spectral efficiency since the subcarriers are overlapped in orthogonal fashion that results in higher transmission data rates and the process is computationally lower with the efficient FFT technique.

Besides, the ISI problem which is commonly occurs in the SCM can be eliminated by introducing the cyclic prefix (CP) (Van Nee and Prasad, 2000). OFDM divides the channel into several narrowband flat fading subchannels which more resilient towards frequency selective fading. Once lost occurs to subcarriers due to channel frequency selectivity, the data can be recovered by using proper channel coder and interleaver (Van Nee and Prasad, 2000). Thus, it provides robust protection against channel interference and impulse noise without implementing an equalizer as in the SCM which reduces the overall system complexity.

Various applications have been utilizing OFDM scheme either in wired or wireless communications. The first application appears in (Weinstein, 2009) where asynchronous digital subscriber line (ADSL) has been introduced, a method of delivering the high-speed data across the phone line. Besides, digital video broadcast - terrestrial (DVB-T) standard (Reimers, 1998) is used in European digital television with standard 8 MHz TV channel, utilizes the subcarriers of 2048 (2K) or 8192 (8K). The other applications include Wireless Local Area Network (WLAN), also known as WiFi (IEEE 802.11a standard) and Worldwide Interoperability for Microwave Access (WiMAX) which is based on IEEE 802.16 standard (Weinstein, 2009).

Nonetheless, the major drawback in OFDM system is high Peak-to-Average Power Ratio (PAPR). This occurs when the peak OFDM signals exceed the threshold and forces the HPA to operate in nonlinear region which causes spectral regrowth of the OFDM signals. Once the orthogonality among the subcarriers are broken, this leads to poor bit error rate (BER) performance at the receiver. Low PAPR allows higher average power to be operated in linear region hence, improving the overall signal-to-noise ratio (SNR) at the receiver.

Furthermore, the application of wavelets or wavelet analysis has been used successfully in many areas such as image processing, signal processing and data compression (Graps, 1995). Due to inherent flexibility in wavelet property of analysis functions with different

time-frequency localization, its performance excels that of Fourier transform when dealing with time-localized signals. Hence, there are applicable in communication systems (Medley et al., 1994). Wavelet packet transform has been chosen for multicarrier modulation (MCM) suitable since its property resembles conventional OFDM system in many cases especially in bandwidth division (Erdol et al., 1995). Wavelet packet-based OFDM also does not require CP hence, bandwidth efficiency can be attained (Kumbasar and Kucur, 2012).

1.2 Problem Statements

MCM scheme is a widely-used transmission technique for delivering massive high-speed data over wireless communication channel. One highlighted issue on MCM scheme is high PAPR of the signal transmission. It also has been identified as a major drawback in common MCM scheme. In another aspect of MCM scheme, traditional approach of achieving orthogonal signals is by applying Fourier transform (i.e. conventional choice). Lately the emergence of wavelet transform, pave the way as a new promising candidate to be utilized in future MCM system. Wavelet has been testified useful for MCM system implementation since it has the merit of possessing orthogonal overlapping symbols in both time and frequency domain. It has been reported in (Kumbasar and Kucur, 2012) that using wavelet removes the need of using the cyclic prefix as in the traditional FFT-OFDM. Hence, this thesis investigates both wavelet-based and wavelet packet-based OFDM systems based on the PAPR profile and BER performance. The selected wavelet-based MCM system will be utilized for further development in PAPR reduction techniques of this thesis.

In order to mitigate PAPR, there have been many techniques proposed in literature either to reduce the peak power with fixed average power or alter the distribution so that the average power produced has smaller peak power (Jiang et al., 2005). Due to this, there are two categories of PAPR reduction techniques which are called as signal distortion technique and signal

scrambling technique. There is a prominent technique which is known as Partial Transmit Sequence (PTS) (Muller and Huber, 1997c). It is categorized as a signal scrambling and has a big potential to be explored and improved.

PTS technique optimizes the MCM frames by scrambling approach in order to find the minimum PAPR value for the operated MCM frame. As a consequences of optimization, the precious residue as known as side information (SI) data is produced. In literature, the management of SI data is not being discussed profoundly. By transmitting the SI data along the corresponding MCM frame to the receiver, an effective signal bandwidth is attainable. Along with this proposed technique, the reconstruction of proposed PTS technique is also discussed with a suggested method is proposed for the PTS reconstruction technique.

1.3 Research objectives

The main objectives in the thesis are:

1. To analyze various wavelet families in their applicability towards MCM systems and their PAPR profiles.
2. To develop PAPR reduction techniques by managing side information (SI) effectively in the partial transmit sequence (PTS) scheme.

1.4 Research Scope

In this work, the MCM system models are assumed to have a ideal signals response between transmitter and receiver and excluding other elements such as synchronization, channel estimation and etc.. The behaviour of system transmission under AWGN channel is analyzed and no multipath propagation is considered. The system focuses on dealing the information bit from the source until the output of orthogonal base modulation at transmitter and for re-

ceiver, starting from input of orthogonal base modulation towards binary recovery. Parts of the MCM systems are analytically performed. Verification of the proposed techniques are done using MATLAB simulations. The works do not involves any hardware prototyping. Figure 1.2 shows the above mentioned processes as indicated red boxes boundaries. Apparently, although the system model is working under baseband frequency, the individual carriers for each sub-carrier are not assigned. Therefore, the bandwidth of the information has no specified limit of operation.

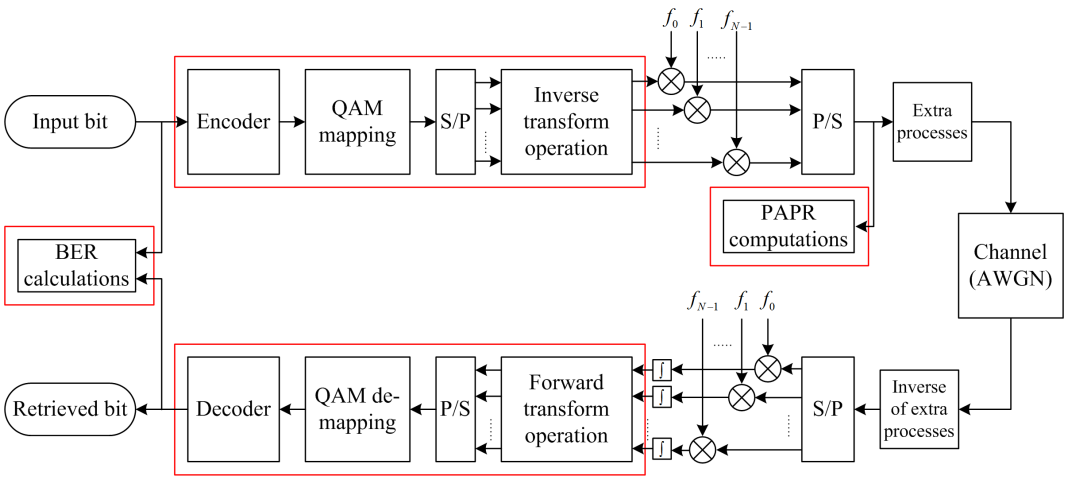

Figure 1.2: Thesis scope (bounded by red boxes)

Analysis is performed on three different orthogonal bases on our MCM system models. They are the Wavelet transform (WT), Wavelet packet transform (WPT) and Fourier transform (FT) as mentioned earlier. Under certain condition, the work testifies the number of subcarriers used as $N = 64, 128$ and 256 with three different symbols constellation mapping which is quadrature amplitude modulation (QAM), 16QAM and 64QAM. By default, the work utilizes the Haar wavelet which also known as Daubechies-1 (length of 2) wavelet. In the specific study on wavelet families such as Symlet and Coiflet wavelets, different length are tested for investigation.

1.5 Research Contribution

Several achieved contributions and original ideas in this thesis are:

1. Comprehensive study on wavelet-based system and wavelet packet-based OFDM system are performed with different parameters for PAPR of MCM signal investigation and its trade-off to BER performance. The incremental changes in the number of subcarriers give small deficit to the PAPR profile but increasing the number of bits per symbol in QAM modulation, causes higher SNR is needed at acceptable BER. Besides, among wavelet families and length, this work proves that the Haar (Daubechies family with length of 2) wavelet is the most suitable wavelet base modulation that can be used in WP-OFDM system.

2. The Proposed PTS Scheme I embeds side information (SI) data into the WP-OFDM frame is successfully achieved. Under limitation of the number of subblock partitions, the PAPR reduction can be achieved. The results are converged to the conventional PTS schemes with small degeneration in BER.

3. The Proposed PTS Scheme II maps the SI based on particular degree of PSK modulation prior embedding the PSK modulated data into the WP-OFDM frame. This results higher number of subblock partitions can be achieved. The BER performance is improved and converged to uncoded one as long as the SI data apply low degree of PSK modulation which relates on the system conditions.

1.6 Thesis Chapters Outline

The thesis is organized as follows. Chapter 2 is divided into two main parts. First part is related to the theoretical, history and background of wavelets, MCM system and PAPR evaluation. Second part describes the research work done on wavelet-based MCM system, in term of PAPR

and BER performance, and research studies on PAPR reduction techniques in general and details.

Chapter 3 presents the analyses of the three type MCM system models which are wavelet-based OFDM, wavelet packet-based OFDM and conventional OFDM as a comparator scheme of the performance. Each part of the system model is explained in details. Among the three schemes, only one is considered to be used in next chapters which focuses more on the PAPR reduction techniques. The combination of the parameters is also included in the summary of the chapter.

Chapter 4 presents the modification on PAPR reduction technique using partial transmit sequence (PTS). Main idea of modification is on dealing the side information (SI) generated after the PTS optimization process. There are two proposed PTS schemes and both are embedding SI data into corresponding MCM frame at the free fixed positions available with *unique* approaches. There are limitations specified in the chapter related to the parameters involved.

Chapter 5 concludes the overall thesis outcomes in previous chapters and list out future works and research recommendations.

CHAPTER 2

LITERATURE REVIEW

This chapter consists of two main parts: First, the history of wavelets, construction of wavelet packet transform, introductory to MCM, wavelet-based MCM systems and method of evaluation for MCM signals by computation of complementary cumulative distribution function (CCDF) for PAPR. Second, reviews all the related recent research works such as the implementation of wavelet-based and wavelet packet-based OFDM systems and several PAPR reduction techniques.

2.1 Background

This section presents the basic background of wavelet analysis, wavelet in multicarrier modulation (MCM) system and overview of CCDF of PAPR. This information is required for the reader to further understand the methodology presented in the next chapters.

2.1.1 Wavelets

The idea of wavelets is derived from the harmonic analysis originated by a French mathematician, J. B. Joseph Fourier (1768-1830). In this concept, any periodic function can be represented as the weighted sum of cosines and sines functions (Fourier trigonometric series). The author also presented the non-periodic time-domain functions in frequency domain by developing Fourier transform (FT). However, Fourier analysis does not function perfectly for every case. It is well-presented in linear problem and stationary signals but in representing the unpredictable of non-stationary signals is quite cumbersome.

Come to the solution, Jean Morlet (1981) introduced the wavelets. His research was on finding for the underground oil using echoes analysis, where it involves the time-frequency analysis. In that work he used the windowed function of FT which is known as short-time Fourier transform (STFT). In that transform a fixed-length Gabor window is used to sweep over the data for analyzing the temporal variations of the spectrum (Gargour et al., 2009). In addition, he found that high frequency signals require short time-domain windows and low frequency signals require long time-domain windows. Thus the weakness of STFT on fixed-length time-domain windows is replaced by stretched and compressed unique oscillating windows by keeping the number of oscillation of window constant. Finally, a dilated and translated function of Morlet wavelet is developed (Kronland-Martinet et al., 1987). The chronology of wavelets for after that time is summarized in Table 2.1 (Gargour et al., 2009; Graps, 1995).

Table 2.1: Chronology of wavelets theory developments

Year	Authors	Descriptions
1981	J. Morlet and A. Grossman	Developed invertible wavelet transformation with perfect reconstruction using coefficients of transformation under certain conditions.
		Modified the wavelet coefficients which leads to denoising operation.
1986	S. Mallat and Y. Meyer	Proposed multiresolution concept in wavelet analysis.
		Constructed Meyer wavelets which they are continuously differentiable but no compact support.
1988	I. Daubechies	Developed a set of wavelet orthonormal basis function which have compact support, continuity and regularity properties, even though does not have smooth and differentiable characteristic.
Post-1990	-	Wavelet theory and application are improved and become versatile tools in many fields.

Wavelets have been used in many fields, including acoustic and speech processing (Kronland-Martinet et al., 1987), image processing (Mallat, 1989a; Antonini et al., 1992; Lee, 2005), medicine and biology (Medl, 1998), magnetic resonance imaging (Healy and Weaver, 1992), physics (Farge et al., 1996) and telecommunications (Moulin et al., 1992; Akansu et al., 1998).

2.1.2 Wavelet Transform

This section presents the basic concept of development of wavelet packet transform (WPT). Basically, WPT is constructed based on the theory of continuous wavelet transform (CWT) and wavelet transform (WT). All the expressions and equations for this subsections are mostly taken and revised from (Li et al., 2010; Torun, 2010; Gargour et al., 2009).

2.1.2(a) Continuous Wavelet Transform (CWT)

The Continuous Wavelet Transform (CWT) is defined as the sum of the signals multiplied by scaling and translation parameters version of a prototype mother wavelet. Using different value of the translation parameter, the wavelet is delayed or hastened from the original wavelet's onset. The value of the translation parameter effects only the location of the wavelet and has no influence neither to duration nor the bandwidth of wavelet. Another important parameter in wavelet is the scaling factor which stretches or compresses the shape of the wavelet. When the scaling factor is increased, wavelet becomes more broaden and therefore has longer time-domain window (suitable for low frequency input signal). If the scaling factor value decreases this causes the wavelet to stretch and therefore has shorter time-domain window (suitable for high frequency input signal). Hence, the scaling factor is inversely proportional to frequency (Torun, 2010).

The CWT of an $L^2(\mathbb{R})$ for signal $x(t)$ is defined as (Daubechies, 1992)

$$X_{\psi_{CWT}}(a,b) = \langle x(t), \psi_{CWT_{a,b}}(t) \rangle = \int_{-\infty}^{+\infty} x(t)\, \psi_{CWT_{a,b}}(t) dt \tag{2.1}$$

where an input signal $x(t)$ is decomposed into a set of wavelet coefficients $X_{\psi_{CWT}}(a,b)$. The parameters a and b denote the scale and translation parameters respectively, which represent new dimension of the wavelet transform. The functions $\psi_{CWT_{a,b}}(t)$ as in Eq. (2.1) are generated using the single mother wavelet $\psi_{CWT}(t)$ given as

$$\psi_{CWT_{a,b}}(t) = \frac{1}{\sqrt{a}} \psi_{CWT}\left(\frac{t-b}{a}\right) \tag{2.2}$$

where $a \in \mathbb{R}^+$ and $b \in \mathbb{R}$ are the scaling and translation parameters respectively. The CWT is a reversible transform. Therefore, the Fourier transform of $\psi_{CWT_{a,b}}(t)$ is given by (Gargour et al., 2009)

$$F\left\{\psi_{CWT_{a,b}}(t)\right\} = \Psi_{CWT_{a,b}}(\Omega) = \sqrt{a}\Psi_{CWT}(a\Omega)e^{-jb\Omega} \tag{2.3}$$

Since the CWT can be considered as the convolution product of the functions $x(t)$ and $\psi(-t/a)$ computed at $t = b$, the Fourier transform of signal $x(t)$ is expressed as

$$F\left(X_{\psi_{CWT}}(a,b)\right) = \sqrt{a}X(\Omega)\psi^*_{CWT}(a\Omega) \tag{2.4}$$

The original signal $x(t)$ can be reconstructed from wavelet coefficient by applying the formulae of inverse wavelet transform

$$x(t) = \frac{1}{C_{\psi_{CWT}}} \int_{a=0}^{+\infty} \int_{b=-\infty}^{+\infty} X_{\psi_{CWT}}(a,b) \frac{1}{a^2} \psi_{CWT} \left(\frac{t-b}{a} \right) da\, db \tag{2.5}$$

where

$$C_{\psi_{CWT}} = \int_{\mathbb{R}^+} \frac{|\Psi_{CWT}(\Omega)|^2}{|\Omega|} d\Omega \tag{2.6}$$

where $\Psi_{CWT}(\Omega)$ denotes the Fourier transform of ψ_{CWT} (Torun, 2010; Gargour et al., 2009).

2.1.2(b) Discrete Wavelet Transform (DWT)

The wavelet coefficients in the CWT are highly redundant, which makes computation takes a huge amount of time and power. Therefore, the usage of discrete wavelets is more suitable and useful in practical problem. The discrete wavelets does not consist of continuous scalable and translatable wavelets, but they are scaled and translated in discrete ways. The discrete scale and translation process of the mother wavelet equation can be written as

$$\psi_{\alpha,\beta} = \sqrt{a_0^{\alpha}} \psi(a_0^{\alpha} t - \beta_{b_0}) \tag{2.7}$$

where a_0 is the fixed step of dilation while b_0 is the translation factor. The integer α and β denote the indices scale and translation respectively. Since the scaling in time corresponds to an inverse scaling in frequency, the product of $(\Delta t_{a,b})(\Delta f_{a,b})$ is independent of the dilation parameter a. As consequences any gain in time resolution is obtained at the cost of the frequency resolution and vice versa. This holds the Heisenberg uncertainty principle for dilated

and translated wavelet $\psi_{CWT_{a,b}}(t)$ as well as for the mother wavelet $\psi_{CWT}(t)$. The dilation step of 2 is the most natural choice which results in octave bands or dyadic scales. For each successive value of scale index, the wavelet is compressed in frequency domain by a factor of 2 and stretched in time domain by the same factor. Translation factor is set to 1 in order to get dyadic sampling. The scaling function and its time-shift set are defined as (Burrus et al., 1997)

$$\varphi_\beta = \varphi(t-\beta), \qquad \beta \in Z, \qquad \varphi \in L^2 \tag{2.8}$$

where Z is the set of all integer numbers, and $L^2(\mathbb{R})$ is the vector space of square integrated function. The parameter v_0 is a space spanned by scaling function, which is defined as

$$v_0 = \overline{\underset{\beta}{Span}\{\varphi_\beta(t)\}}, \qquad \beta \in Z \tag{2.9}$$

In this subspace, if $x(t) \in v_0$, it can be expressed as

$$x(t) = \sum_{\beta=-\infty}^{+\infty} a_\beta \varphi_\beta(t) \tag{2.10}$$

One can increase the size of the subspace by changing the time scale of the scaling functions. The two-dimensional parameterization (time and scale) of scaling function $\varphi(t)$ from v_0 to v_α can be expressed as

$$\varphi_{\alpha,\beta} = 2^{\alpha/2}\varphi(2^\alpha t - \beta) \tag{2.11}$$

Then, the new function for the expanded subspace v_α is given as

$$v_\alpha = \overline{\underset{\beta}{Span}\{\varphi_\beta(2^\alpha t)\}} = \overline{\underset{\beta}{Span}\{\varphi_{\alpha,\beta}(t)\}} \tag{2.12}$$

In the extended subspace, whenever $x(t) \in v_\alpha$, then it can be expressed as

$$x(t) = \sum_{\beta=-\infty}^{+\infty} a_\beta \varphi(2^\alpha t + \beta) \tag{2.13}$$

Looking at the Eq. (2.13), for $\alpha > 0$ the span v_α is larger than v_0, and $\varphi_{\alpha,\beta}(t)$ can represent finer detail since it has the finer scale while for $\alpha < 0$ it is true for coarse scale. Wavelet conforms to the requirement of multi-resolution concept. In this concept, every signal is decomposed into finer detail in gradual fashion (Akansu and Haddad, 1992). The basic form of multi-resolution analysis (MRA) requirement, given by (Mallat, 1989a)

$$\cdots \subset v_{-2} \subset v_{-1} \subset v_0 \subset v_1 \subset v_2 \subset \cdots \subset L^2 \tag{2.14}$$

where $v_{-\infty} = \{0\}$ and $v_{+\infty} = L^2$, means that within a same vector space of L^2, it contains both high resolution and low resolution coefficients. Hence, if $x(t) \in v_\alpha$, then $x(2t) \in v_{\alpha+1}$. The term of $\varphi(t)$ can be expressed as the weighted sum of the time-shifted scaling function

$$\varphi(t) = \sum_{n=-\infty}^{+\infty} h(n)\sqrt{2}\varphi(2t-n), \qquad n \in Z \tag{2.15}$$

where $h(n)$ is the scaling function coefficients in the form of a sequence of real or imaginary

numbers. The expanded space for v_α is $v_{\alpha+1}$ and its orthogonal complement is defined as w_α. Thus, this produces a new set of spaces. Let the subspace is spanned by the wavelet be $w_{\alpha+1}$, then the expansion of v_1 and v_2 can be written as

$$\begin{aligned} v_1 &= v_0 \oplus w_0 \\ v_2 &= v_1 \oplus w_1 = (v_0 \oplus w_0) \oplus w_1 \\ &\vdots \\ v_{\alpha+1} &= v_\alpha \oplus w_\alpha = v_0 \overset{\alpha}{\underset{l=0}{\oplus}} w_l, \qquad \forall \alpha \in Z \end{aligned} \tag{2.16}$$

which is clearly depicted in Figure 2.1 (Li et al., 2010).

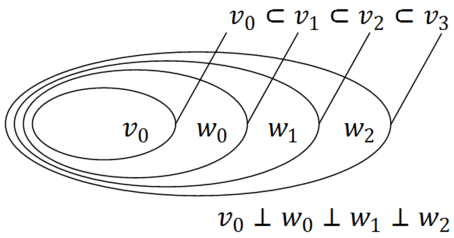

Figure 2.1: Wavelet vector spaces and scaling function

Next, the wavelet function $\psi(t)$ is defined similar to scaling space v_0. Let w_0 represents the space spanned by the wavelet function $\psi_\beta(t)$ and the expanded space as w_α spanned by $\psi_{\alpha,\beta}(t)$ using Eq. (2.9) to Eq. (2.12). The w_α term is orthogonal to v_α and the orthogonality between $\varphi(t)$ and $\psi(t)$ is given as (Li et al., 2010)

$$\langle \varphi_{\alpha,\beta}(t), \psi_{\alpha,\beta}(t) \rangle = \int \varphi_{\alpha,\beta}(t) \psi_{\alpha,\beta}(t) dt = 0 \tag{2.17}$$

Due to these wavelets are in space spanned by the next finer scaling function, the wavelet function $\psi(t)$ can be expressed by the sum of the weighted time-shifted wavelet function given as

$$\psi(t) = \sum_{n=-\infty}^{+\infty} g(n)\sqrt{2}\varphi(2t-n), \qquad n \in Z \tag{2.18}$$

where $g(n)$ is called the wavelet function coefficient. The relationship between wavelet filter $g(n)$ and scaling filter $h(n)$ can be expressed as (Li et al., 2010)

$$g(n) = (-1)^n h(1-n) \tag{2.19}$$

Both coefficients are restricted by the orthogonality condition. If $h(n)$ has a finite even length N, then the Eq. (2.19) can be rewritten as

$$g(n) = (-1)^n h(N-1-n) \tag{2.20}$$

It is well known that an orthonormal perfect reconstruction (PR) always requires the wavelet function coefficients $g(n)$. Here PR gives the advantage to a communication system so that the received signals at the receiver can be reconstructed perfectly. As for an example, let analyze the Haar wavelet below. The wavelet function $\psi(t)$ for Haar is given as

$$\psi(t) = \begin{cases} 1 & 0 \le t \le 0.5 \\ -1 & 0.5 \le t \le 1 \\ 0 & \text{otherwise} \end{cases} \tag{2.21}$$

and its scaling function is

$$\varphi(t) = \begin{cases} 1 & 0 \leq t \leq 1 \\ 0 & \text{otherwise} \end{cases} \tag{2.22}$$

Furthermore, the basic version of Haar wavelet for wavelet and scaling function is shown in Figure 2.2.

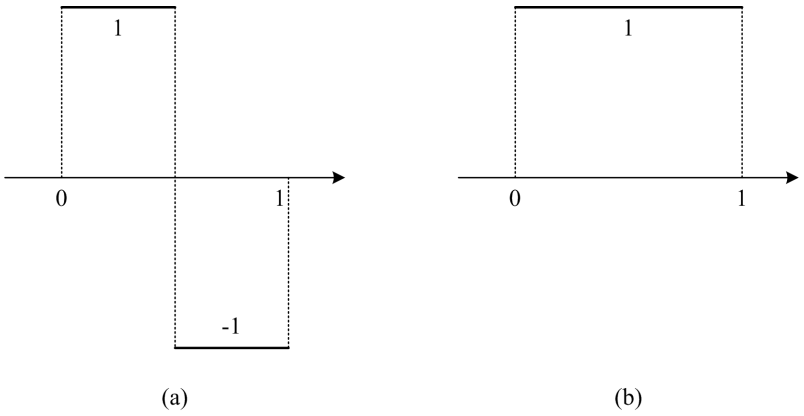

(a) (b)

Figure 2.2: Haar wavelet

The Haar filter coefficients are obtained by applying Eq. (2.15) and Eq. (2.18).

$$g(n) = \left(\frac{1}{\sqrt{2}}, \frac{-1}{\sqrt{2}} \right) \tag{2.23a}$$

$$h(n) = \left(\frac{1}{\sqrt{2}}, \frac{1}{\sqrt{2}} \right) \tag{2.23b}$$

Until to this point, the wavelet and scaling functions (i.e. $\psi_{\alpha,\beta}(t)$ and $\varphi_{\alpha,\beta}(t)$) as well as example of wavelet and scaling function coefficients (i.e. $g(n)$ and $h(n)$ are presented. Furthermore, the discrete wavelet expansion of any signal $x(t) \in L^2(\mathbb{R})$ can be expressed as (Torun, 2010)

$$x(t) = \sum_{\beta=-\infty}^{+\infty} c_{\alpha_0}(\beta)\varphi_{\alpha_0,\beta}(t) + \sum_{\beta=-\infty}^{+\infty} \sum_{\alpha=\alpha_0}^{+\infty} d_{\alpha}(\beta)\psi_{\alpha,\beta}(t) \tag{2.24}$$

for $\alpha, \beta \in Z$ which Z is real integer, $L^2(\mathbb{R})$ is the vector space of square integrated function, and α_0 is an arbitrary integer. It shows that α and β provide the frequency (or scale) and time localizations respectively.

Given that, the term $c_\alpha(\beta)$ is known as the approximation coefficient while $d_\alpha(\beta)$ is known as the detail coefficient. In the wavelet expansion, the higher scale of $\alpha+1$ can also be obtained by manipulating Eq. (2.15) and Eq. (2.18) produces the approximation coefficient as

$$\begin{aligned} c_\alpha(\beta) &= \langle x(t), \varphi_{\alpha,\beta}(t) \rangle \\ &= \int x(t) 2^{\alpha/2} \varphi(2^\alpha t - \beta) dt \\ &= \sum_m h(m-2\beta) c_{\alpha+1}(m) \end{aligned} \tag{2.25a}$$

and the detail coefficient as

$$\begin{aligned} d_\alpha(\beta) &= \langle x(t), \psi_{\alpha,\beta}(t) \rangle \\ &= \int x(t) 2^{\alpha/2} \psi(2^\alpha t - \beta) dt \\ &= \sum_m g(m-2\beta) c_{\alpha+1}(m) \end{aligned} \tag{2.25b}$$

Equation (2.25a) and Eq. (2.25b) show the scaling and wavelet DWT coefficients respectively. The terms of $c_\alpha(\beta)$ and $d_\alpha(\beta)$ can be computed by taking weighted the sum of DWT coefficients of higher scale $\alpha+1$. To obtain scaling DWT coefficients at scale α, $c_\alpha(\beta)$ there is a convolution between scaling function coefficient, $h(n)$ and scaling DWT coefficients at scale $\alpha+1$, $c_{\alpha+1}(\beta)$ and continuing with subsampling with factor 2. While to get wavelet DWT coefficients at scale α, $d_\alpha(\beta)$ the convolution between wavelet function coefficient, $g(n)$ and scaling DWT coefficients at scale $\alpha+1$, $c_{\alpha+1}(\beta)$ is performed and continuing with subsampling with factor 2. Hence, both expressions can be viewed as the 2-channel analysis filter banks as in Figure 2.3 (Goswami and Chan, 2011).

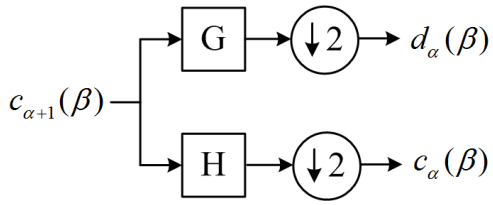

Figure 2.3: Single level DWT decomposition

The 2-channel filter bank splits the input signal in two portions and filters first portion with filter H and second one with filter G. The filtered signals are subsampled by 2 then. Each output signal will possess half number of samples and will span half of the frequency band compared to original signal. Since two filters are used, the number of samples at the output filter bank is similar to the number of samples at the input. The decomposition process starts with $c(\beta)$ at the largest scale. If there is $c_3(\beta)$, this implies the number of decomposition involved is three, which finally produces $c_0(\beta)$, $d_0(\beta)$, $d_1(\beta)$ and $d_2(\beta)$ at the terminal of the decomposition branches, as shown in Figure 2.4.

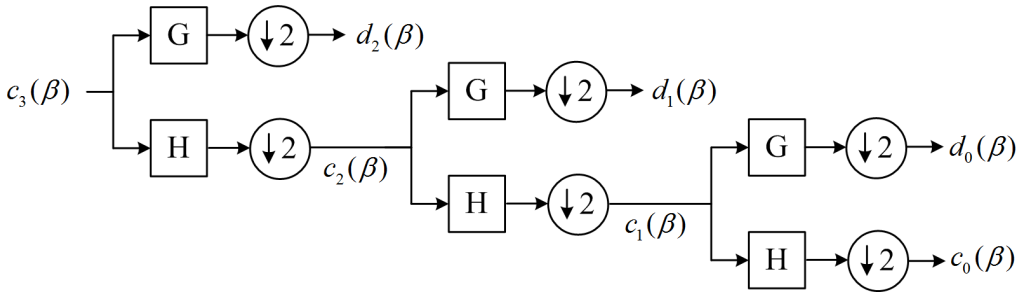

Figure 2.4: Three level DWT decomposition

Furthermore, the reconstruction for given DWT coefficients is given in Eq. (2.24). If the refinement equations for scaling (Eq. (2.15)) and wavelet function (Eq. (2.18)) are substituted into the reconstruction function in Eq. (2.24), it produces

$$
\begin{aligned}
x(t) &= \sum_{\beta=-\infty}^{+\infty} c_{\alpha_0}(\beta)\varphi_{\alpha_0,\beta}(t) + \sum_{\beta=-\infty}^{+\infty}\sum_{\alpha=\alpha_0}^{+\infty} d_{\alpha}(\beta)\psi_{\alpha,\beta}(t) \\
&= \sum_{\beta=-\infty}^{+\infty} c_{\alpha_0}(\beta) \sum_{n=-\infty}^{+\infty} h(n)(\sqrt{2})^{\alpha+1}\varphi(2^{\alpha+1}-2\beta-n) \\
&\quad + \sum_{\beta=-\infty}^{+\infty}\sum_{\alpha=\alpha_0}^{+\infty} d_{\alpha}(\beta) \sum_{n=-\infty}^{+\infty} g(n)(\sqrt{2})^{\alpha+1}\varphi(2^{\alpha+1}-2\beta-n)
\end{aligned} \tag{2.26}
$$

By multiplying both sides of Eq. (2.26) with $\varphi(2^{\alpha+1}-\beta)$ and taking the integral produces the lower scale of DWT coefficients (Mallat, 1989b), the scaling DWT coefficients of higher scale is

$$
c_{\alpha+1}(\beta) = \sum_m c_{\alpha}(m)h(\beta-2m) + \sum_m d_{\alpha}(m)g(\beta-2m) \tag{2.27}
$$

This implies that scaling DWT coefficients at a certain level $\alpha+1$ can be computed by taking the weighted wavelet DWT coefficients and scaling DWT coefficients of scale α. This process is called 2-channel synthesis filter bank as depicted in Figure 2.5. The scaling and wavelet DWT coefficients at scale α are first upsampled by factor 2 and subsequently scaling DWT coefficients are filtered with LPF $\hat{H}$ while wavelet DWT coefficients are filtered with HPF $\hat{G}$. The two filtered signals are added together to form scaling DWT coefficients at scale $\alpha+1$.

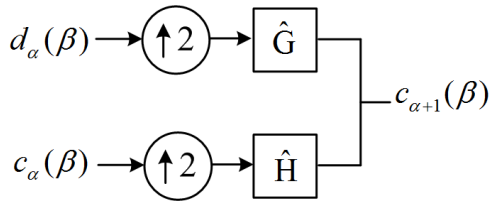

Figure 2.5: Single level DWT reconstruction

The discrete wavelet transform (DWT) decompose a signal into coefficients. The inverse discrete wavelet transform (IDWT) reconstructs the original signal from coefficients. The IDWT can be implemented efficiently by iterating the 2-channel synthesis filter bank.

2.1.2(c) Wavelet Packet Transform (WPT)

In DWT decomposition, the iteration of the 2-channel filter bank is performed only towards the low pass branch direction. At the end of decomposition, the low frequencies portion possesses the narrow bandwidth due to fewer numbers of coefficients while high frequencies will have a wide bandwidth since have many numbers of coefficients. In comparison to wavelet packet transform (WPT), the iteration of 2-channel filter bank is performed on both sides, which are at low pass and high pass branches. As both the high frequency and low frequencies components are decomposed, the WPT has evenly space frequency resolution and similar bandwidth size.

The filter bank structure for WPT expands into a full binary tree. A set of WPT coefficients is labelled by ζ and the level which corresponds to depth of the node in the tree is indicated by l and the position at current node by p. The WPT splits every parent node in two orthogonal subspace W_l^p located at the next level recursively as (Li et al., 2010)

$$W_l^p = W_{l+1}^{2p} \oplus W_{l+1}^{2p+1}, \qquad W_l^p = \overline{Span\{2^{l/2}\zeta_l^p(2^l t - \beta)\}} \tag{2.28}$$

In WPT, the scaling WPT coefficients are denoted as ζ_{l+1}^{2p} and wavelet WPT coefficients are labelled as ζ_{l+1}^{2p+1}. The function of both term is given in Eq. (2.29) and depicted in Figure 2.6.

$$\zeta_{l+1}^{2p}(\beta) = \sum_m h(m-2\beta)\zeta_l^p(m) \tag{2.29a}$$

$$\zeta_{l+1}^{2p+1}(\beta) = \sum_m g(m-2\beta)\zeta_l^p(m) \tag{2.29b}$$

In WPT, the number of iteration by 2-channel filter bank is increased exponentially as the number of level is increased. Therefore, WPT has higher computational complexity than

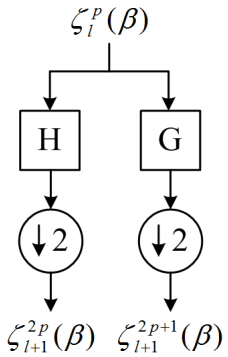

Figure 2.6: WPT decomposition at single level

regular DWT. By using fast filter bank algorithm, WPT requires $O(Nlog(N))$ operation, while FFT needs only $O(N)$ calculation in DWT (Burrus et al., 1997). The reconstruction of WPT is executed by taking tree reverse version of Figure 2.6. The wavelet packet coefficients at level l is given as

$$\zeta_l^p(\beta) = \sum \zeta_{l+1}^{2p}(m)h(\beta - 2m) + \sum \zeta_{l+1}^{2p+1}(m)g(\beta - 2m) \tag{2.30}$$

2.1.3 Multicarrier Modulation (MCM) System

A special multicarrier modulation (MCM) schemes was firstly introduced by Chang (1966) for modulating signals with higher spectral efficiency by transforming the single high-speed serial signal into multiple low-speed parallel signals with N overlapping subcarriers. This type of MCM is known as orthogonal frequency division multiplexing (OFDM) and it is widely applied in many applications such as in European Digital Audio Broadcasting (DAB), IEEE 802.11 (WiFi) and IEEE 802.16 (WiMAX). OFDM has high spectral efficiency due to its overlapping subcarriers applies the orthogonality concept. Consecutive subcarriers cause no crosstalk as long as the orthogonality is preserved.

Generally, this thesis describes wavelet-based MCM for both types of systems i.e. wavelet-based OFDM (WOFDM) and wavelet packet-based OFDM (WP-OFDM) systems and this term

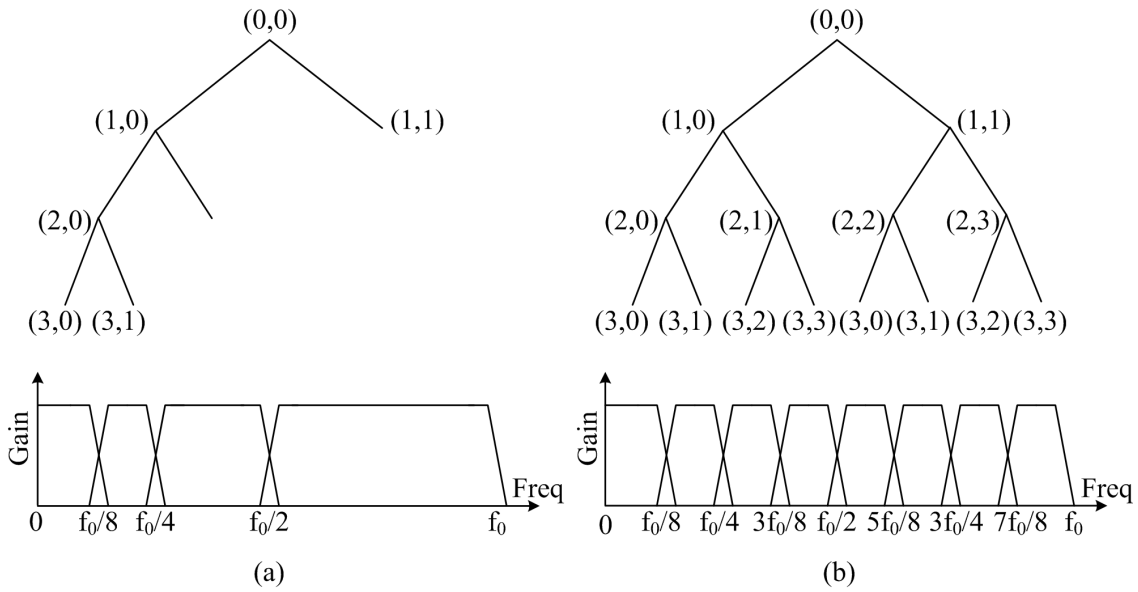

Figure 2.7: Decomposition and bandwidth division for (a) DWT and (b) WPT

is used throughout the thesis. It is clearly observed that the primary difference between those two is the way of wavelet tree is being expanded. Wavelet decomposition expands its branches in dyadic way while wavelet packet decomposition expands in each node as full binary tree. Hence, wavelet packet possesses richer signal analysis than wavelets and capable to focus on any tree nodes in for detail analysis. This main difference of wavelet-based MCM systems is depicted in Figure 2.7. Notice that the implication of wavelet decomposition produces different range of bandwidth division. Wavelet bandwidth is in form on dyadic division while wavelet packet has uniform bandwidth division. In multicarrier communication, the use of wavelet transform (WT) is not suitable and the best wavelet-based MCM is WP-OFDM since the majority characteristic of this scheme resemble the conventional OFDM (Erdol et al., 1995) i.e. bandwidth division for speciality.

Wavelet packet-based OFDM (WP-OFDM) is a scheme that utilizes wavelet packet bases to operate a series of parallel signals into single composite signal. Indeed, both OFDM and WP-OFDM have several similarities especially in term of possessing high spectral efficiency since make use of orthogonal base for allowing subcarriers to overlap each other in conditions. The difference between both schemes is the shape of the subcarriers produced. OFDM utilizes